ACID SULFATE ALTERATION PRODUCTS OF A THOLEIITIC BASALT: IMPLICATIONS FOR INTERPRETATION OF MARTIAN THERMAL EMISSION SPECTRA. R. V. Morris[1], T. Graff[2], M. D. Lane[1], D. C. Golden[2], C. S. Schwandt[2], T. D. Shelfer[2], D. W. Ming[1], S. A. Mertzman[3], J. F. Bell III[4], J. Crisp[5], and P. R. Christensen[6], [1]SN/NASA Johnson Space Center, Houston TX 77058 (richard.v.morris1@jsc.nasa.gov), [2]Lockheed Martin Space Operations, Houston, TX 77058, [3]Dept. of Geosciences, Franklin and Marshall College, Lancaster, PA, [4]Dept. of Astronomy, Cornell University, Ithaca, NY, [5]Jet Propulsion Laboratory, Pasadena, CA, [6]Dept. of Geology, Arizona State University, Tempe, AZ.

Introduction. The high concentration of SO_3 (~7% [1]) in martian soil implies that acid sulfate alteration, possibly driven by SO_2 associated with volcanic exhalations [e.g., 2], was an active alteration process on Mars and possibly is still ongoing. Despite the high elemental concentration of sulfur, observational spectroscopic evidence for specific sulfur-bearing minerals (presumably sulfates) on Mars has been elusive [e.g., 3]. We are doing chemical and mineralogical studies of a tholeiitic basalt rock that has undergone active acid sulfate weathering in order to identify the alteration products, their distribution in the rock, and their expected manifestation in martian remote sensing data. We consider here major element, pH, X-ray diffraction (XRD), and thermal emission data.

Sample. Tholeiitic basalt HWSB820 is an equidimensional rock ~10 cm on a side. It was partially buried in soil (~2 cm exposed), within 10 m of an active fumarole at Sulfur Bank, Hawaii. Three adjacent sides, including the top surface were relative smooth and heavily altered as indicated by their light color. The other three sides were irregular, much darker (less altered) surfaces. A vertical saw cut through the rock showed a gradation in color (top to bottom) from white to grey to black; vesicles and amygdules were common on the sawed surfaces. We obtained two adjacent square cores (~3 cm cross section) by sawing through the center of the rock normal to the top surface. Each core was then sawed at the same locations perpendicular to the core axis to obtain nine rock slabs ~1 cm thick. One set of slabs was ground to fine powders for major element, pH, and XRD measurements. The other set of slabs was used for thermal emission measurements. Methods are described by [4,5,6,7].

Results and Discussion. Major element concentrations and pH values for selected slabs (Table 1) show an extreme elemental variation and an acid pH (~4-5) consistent with active acid-sulfate alteration. The uppermost slab (S3-1) has >90% SiO_2. The SiO_2 concentration decreases with depth to a relatively constant ~54% by slab S3-5. The slab that includes the bottom rock surface (S3-9) is also somewhat enriched in SiO_2. The high volatile contents (LOI ~9-16%) and Fe_2O_3/FeO >1 for all slabs show that all regions of the rock have been altered.

XRD patterns are shown in Fig. 1a. The uppermost slab is dominated by the broad line centered near 23° 2θ for X-ray amorphous (nanophase) $SiO_2.nH_2O$. All the sharp peaks belong to anatase (TiO_2 polymorph). In the next slab, nanophase $SiO_2.nH_2O$ is still present, and all the sharp lines are natroalunite $(NaAl_3(SO_4)_2(OH)_6$. In the third slab (S3-3), diffraction lines for the rock forming minerals plagioclase feldspar and pyroxene are present for the first time and the intensity of the nanophase $SiO_2.nH_2O$ peak decreases markedly. Also present is gypsum ($CaSO_4.2H_2O$). In subsequent slabs, gypsum, natroalunite, feldspar, and pyroxene account for all the major XRD peaks. Note that the broad nanophase $SiO_2.nH_2O$ peak has increased in intensity in the bottom slab (S3-9) relative to slabs closer to the top.

Table 1. Average depth (in cm) beneath top rock surface and values of pH and major element composition of ~1 cm thick slabs cut parallel to the rock surface.

	S3-1	S3-2	S3-3	S3-5	S3-7	S3-9
Depth	0.45	1.50	2.55	4.75	6.80	9.15
pH	3.94	3.96	4.53	5.24	5.00	4.60
SiO_2	90.72	82.37	62.39	53.41	53.93	62.25
TiO_2	4.62	4.02	3.13	2.51	2.54	3.22
Al_2O_3	2.82	7.47	13.83	17.47	16.98	14.48
Fe_2O_3T	0.92	3.61	9.64	10.52	10.50	10.23
MnO	0.01	0.03	0.10	0.12	0.13	0.10
MgO	0.08	0.21	3.82	4.99	5.24	3.11
CaO	0.22	0.30	4.68	8.18	7.99	4.22
Na_2O	0.00	0.65	1.33	1.79	1.69	1.34
K_2O	0.12	0.35	0.31	0.22	0.22	0.28
P_2O_5	0.14	0.33	0.34	0.31	0.29	0.36
Total	99.65	99.34	99.57	99.52	99.51	99.59
LOI	10.70	16.42	14.93	11.59	9.63	14.12
FeO	0.27	0.72	3.25	3.98	4.41	3.50
Fe_2O_3	0.62	2.81	6.03	6.10	5.60	6.34

Thermal emission spectra for slab top surfaces are given in Fig. 1b. The spectrum labeled S2-1 is thus the exposed rock surface. Although the intensity of the features changes, the S1-1, -2, and -3 emissivity spectra are the same and characterized by emissivity minima near 1105 and 470 cm^{-1} and a shoulder near 1240 cm^{-1}. We believe all these features result from nanophase $SiO_2.nH_2O$ because it is the only XRD phase common to all three samples, and it is X-ray amorphous like glass and has an emissivity spectrum very similar to that for high-SiO_2 obsidian glass (Fig. 1b).

Our nanophase $SiO_2.nH_2O$ emissivity spectrum is essentially equivalent to the mid-IR spectra published by [8,9,10] for the surfaces of weathered Mauna Loa lavas. They attribute the appearance of the 1105 cm^{-1}

feature mentioned above to rearrangement (organization) of silica tetrahedra within glass as it matures. However, our nanophase $SiO_2.nH_2O$ is not a glass derived by rapid cooling of a silicate liquid. It is better characterized as a nanophase precipitation product from small-volume acid sulfate solutions within cavities and along fractures and grain boundaries in the rock. This view is consistent with the relative insolubility of anatase and natroalunite. We suggest that [8,9,10] are also detecting, on a smaller scale, these $SiO_2.nH_2O$ precipitation products on lava surfaces.

The spectral signature of $SiO_2.nH_2O$ is not readily apparent in the last three emissivity spectra. Instead, the signature of the silicate minerals dominates. Just visible, however, is a weak band at 675 cm^{-1} which corresponds to a gypsum emissivity feature (Fig. 1b). The more intense gypsum feature at 1159 cm^{-1} probably defines the high wavenumber edge of the envelope centered on ~1000 cm^{-1} that contains the silicate emissivity features.

Application to Mars. If acid sulfate alteration (or any process that leads to dissolution of rock and precipitation of nanophase $SiO_2.nH_2O$) occurs on martian rock surfaces, it might have a pattern like those of slab spectra S2-1 through S2-3. In any event, it might not be possible to distinguish between glass like obsidian and nanophase $SiO_2.nH_2O$ because of the near correspondence of their emissivity spectra (Fig. 1b). The distinction is important because of the drastically different genetic implications of glass versus nanophase $SiO_2.nH_2O$.

In martian emissivity spectra, the 550-800 cm^{-1} region is excluded for analysis of surface materials because of atmospheric CO_2 [e.g., 6]. If this restriction were applied to spectra in Fig. 1b, gypsum could not be identified by the 675 cm^{-1} feature and it is questionable its presence could be inferred from the remainder of the spectrum. A corollary is that it will be difficult to identify gypsum as the sulfate on Mars if gypsum and silicate features are comparable as in the S2-5 and S2-7 emissivity spectra.

References: [1] Rieder et al., *Science, 278*, 1771, 1997; [2] Settle, *JGR, 84*, 8343, 1979; [3] Bell, *Min. Spec.: A Tribute to RG Burns*, Geochem. Soc. Spec. Pub. 5, 1996; [4] Morris et al., *JGR*, in press, 2000; [5] Ruff et al., *JGR, 102*, 14,899, 1997; [6] Christensen et al., *JGR*, in press, 2000; [7] Jackson, *Soil Chemical Analysis - Advanced Course*, published by the author, 1985; [8] Kahle et al., *JGR, 93*, 15,239, 1988; [9] Crisp et al., *JGR, 95*, 21657, 1990; [10] Kahle et al., *Geophys. Mono. 92*, 145, 1995.

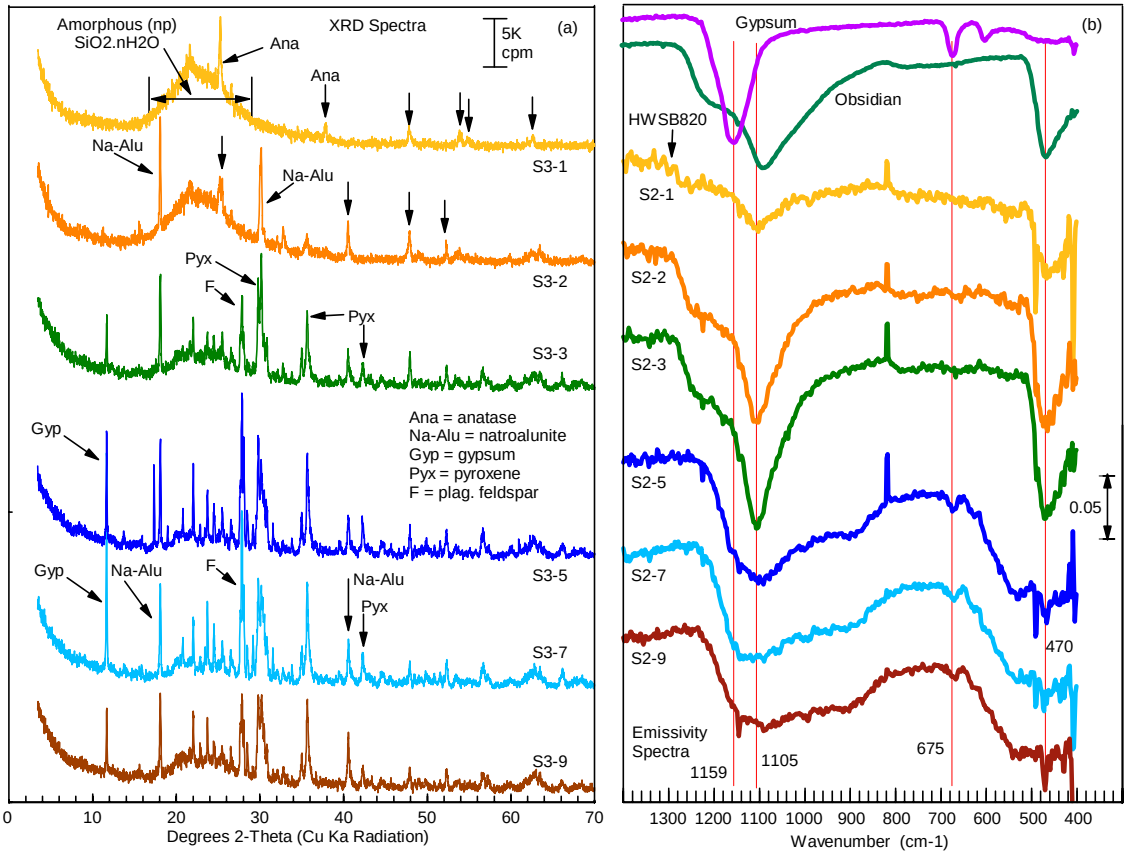

Figure 1 (left). XRD spectra of powders of slabs that correspond to the emissivity spectra in Fig. 2.
Figure 2 (right). Emissivity spectra for slab tops. Spectra of gypsum and obsidian shown for comparison.